The role of imaging in the detection and management of COVID-19: a review

Di Dong, Zhenchao Tang, Shuo Wang, Hui Hui, Lixin Gong, Yao Lu, Zhong Xue, Hongen liao, Fang Chen, Fan Yang, Ronghua Jin, Kun Wang, Zhenyu Liu, Jingwei Wei, Wei Mu, Hui Zhang, Jingying Jiang, Jie Tian, *Fellow, IEEE*, Hongjun Li

***Abstract*—Coronavirus disease 2019 (COVID-19) caused by the severe acute respiratory syndrome coronavirus 2 (SARS-CoV-2) is spreading rapidly around the world, resulting in a massive death toll. Lung infection or pneumonia is the common complication of COVID-19, and imaging techniques, especially computed tomography (CT), have played an important role in diagnoses and treatment assessment of the disease. Herein, we review the use of imaging characteristics and computing models that have been applied for the management of COVID-19. CT, positron emission tomography - CT (PET/CT), lung ultrasound, and magnetic resonance imaging (MRI) have been used for detection, treatment, and follow-up. The quantitative analysis of imaging data using artificial intelligence (AI) is also explored. Our findings indicate that typical imaging characteristics and their changes can play an important role in the detection and management of COVID-19. In addition, AI or other quantitative image analysis methods are urgently needed to maximize the value of imaging in the management of COVID-19.**

***Index Terms*—COVID-19, imaging, chest CT, artificial intelligence**

This work was supported by the National Natural Science Foundation of China (81930053, 91959130, 81971776, 81771924, 81227901, 81671851, 81827808, 81527805), National Key R&D Program of China (2017YFA0205200, 2017YFC1308700, 2017YFC1309100, 2017YFA0700401, 2016YFC0103803), the Beijing Natural Science Foundation (L182061), and the Youth Innovation Promotion Association CAS (2017175), the Strategic Priority Research Program under Grant XDB32030200 and the Scientific Instrument R&D Program under Grant YJKYYQ20170075 of the Chinese Academy of Sciences. (D. Dong, Z. Tang, S. Wang, H. Hui, L. Gong, and Y. Lu contributed equally as co-first authors.) (Corresponding authors: J. Tian, H. Li).

D. Dong, H. Hui, K. Wang, Z. Liu, and J. Wei are with School of Artificial Intelligence, University of Chinese Academy of Sciences, Beijing, China, and with CAS Key Laboratory of Molecular Imaging, Institute of Automation, Chinese Academy of Sciences, Beijing, China. Z. Tang, S. Wang, W. Mu, H. Zhang, and J. Jiang are with Beijing Advanced Innovation Center for Big Data-Based Precision Medicine, School of Medicine and Engineering, Beihang University, and with Key Laboratory of Big Data-Based Precision Medicine (Beihang University), Ministry of Industry and Information Technology, Beijing, China. L. Gong is with College of Medicine and Biological Information Engineering School, Northeastern University. Y. Lu is with School of Data and Computer Science, Sun Yat-sen University, Guangzhou, China. Z. Xue is with Shanghai United Imaging Intelligence Co Ltd, Shanghai, China. H. Liao and F. Chen are with Department of Biomedical Engineering, School of Medicine, Tsinghua University, Beijing, China. F. Yang is with Department of Radiology, Union Hospital, Tongji Medical College, Huazhong University of Science and Technology, Wuhan, China. R. Jin is with Beijing Youan Hospital, Capital Medical University, Beijing, China. J. Tian is with CAS Key Laboratory of Molecular Imaging, Institute of Automation, Chinese Academy of Sciences, Beijing 100190, China, and with Beijing Advanced Innovation Center for Big Data-Based Precision Medicine, School of Medicine and Engineering, Beihang University, China (email: tian@ieee.org). H. Li is with Department of Radiology, Beijing Youan Hospital, Capital Medical University, Beijing, 100069, China (email: lihongjun00113@126.com).

I. Introduction

Coronavirus disease 2019 (COVID-19), which is caused by the severe acute respiratory syndrome coronavirus 2 (SARS-CoV-2), emerged in December 2019 and rapidly developed into a global outbreak [1, 2]. COVID-19 presents as an acute respiratory tract infection syndrome and is highly infectious [3]. Critically ill patients with COVID-19 have a high mortality rate [4]. By April 20, 2020, more than 84,000 COVID-19 cases have been confirmed in China and more than 2.30 million cases globally.

The typical clinical characteristics of COVID-19 cases include fever, respiratory symptoms, pneumonia, decreased white blood cell (WBC) count, or decreased lymphocyte count [5-7]. The reverse-transcription polymerase chain reaction (RT-PCR) testing is considered as the standard method for screening suspected cases [8, 9]. However, the sensitivity of RT-PCR screening is relatively poor. Thus, SARS-CoV-2 infection cannot be entirely excluded, even if RT-PCR results from a suspected patient are negative [10-12]. Therefore, medical imaging, in particular, chest computed tomography (CT), is often used as a complementary examination in the diagnosis and management of COVID-19. Typical imaging characteristics of lung in COVID-19 include lesions with ground-glass opacities (GGO), lung consolidation, bilateral patchy shadowing, pulmonary fibrosis, multiple lesions and crazy-paving pattern, and so on [13, 14]. These imaging interpretations played a key role not only in the diagnosis and treatment of COVID-19 but also in the monitoring of disease progression and the evaluation of therapeutic efficacy [15, 16].

The latest Chinese diagnosis and treatment protocol for COVID-19 (trial version 7) also highlights the value of imaging for detecting COVID-19 [9]. As shown in the flowchart of COVID-19 detection and staging of adult patients in China (Figure 1), chest imaging has played an important role in both the case definition and clinical classification of COVID-19.

Case definitions: For screening of the suspected cases, the epidemiological history and clinical manifestations of a patient are comprehensively analyzed, in which the chest imaging characteristics is adopted as one of the clinical manifestations [9]. Abnormal chest imaging characteristics of COVID-19 include multiple small patchy shadows and interstitial changes, more apparent in the peripheral zone of lungs (early stage), multiple ground glass opacities and infiltration in both lungs (progression stage), pulmonary consolidation (severe stage). A

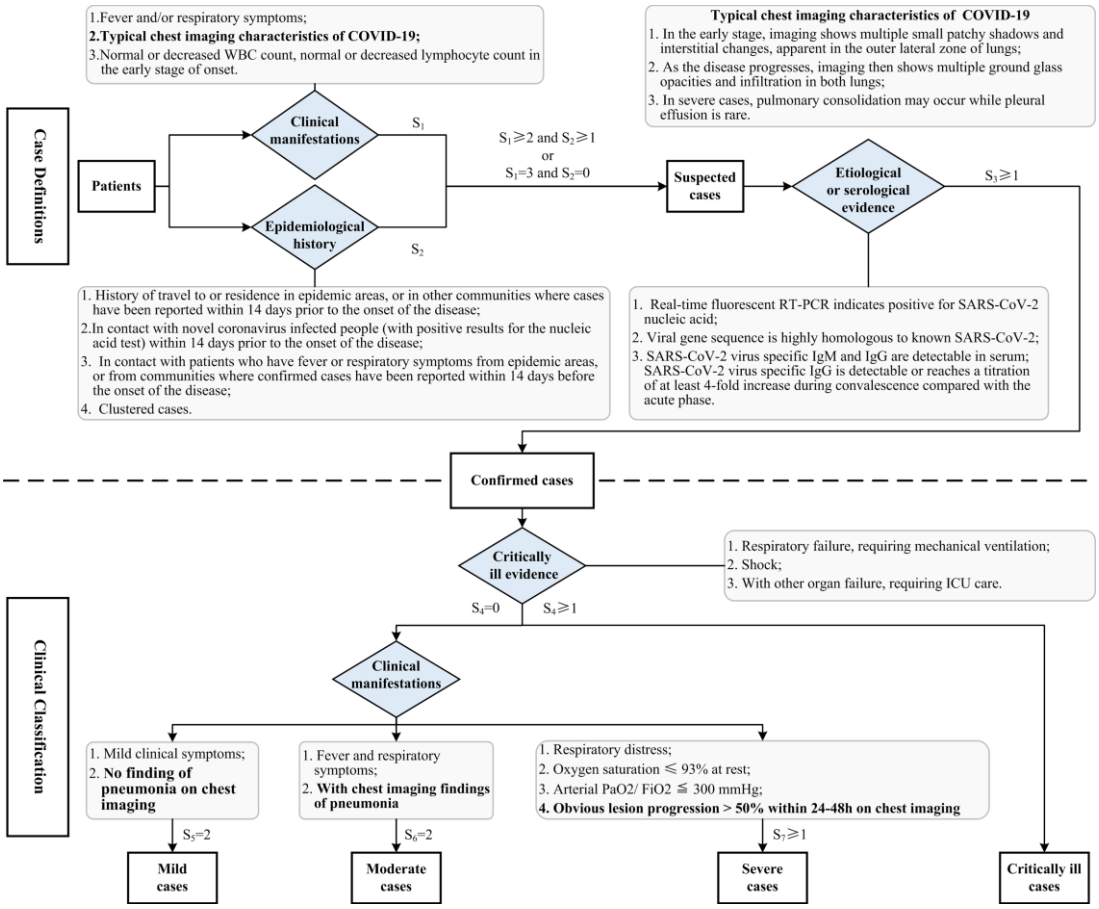

Figure 1. The flowchart of case definitions and clinical staging of adult patients in China [9]. S: the number of entries that meet the conditions.

suspected case with any positive etiological or serological results is confirmed as COVID-19.

Clinical classification: Confirmed COVID-19 cases are classified as mild, moderate, severe, or critically ill cases. The classifications of the first three types all involve the chest imaging. COVID-19 cases with mild clinical symptoms and with no sign of pneumonia on chest imaging are confirmed as mild cases, while cases with fever, respiratory symptoms, and chest imaging findings of pneumonia are categorized as moderate cases. Besides the respiratory distress, oxygen saturation, and arterial partial pressure of oxygen (PaO2)/fraction of inspired oxygen (FiO2), an adult case with chest imaging showing obvious lesion progression >50% within 24-48 hours should be managed as a severe case.

There are lots of studies investigating the imaging characteristics during the diagnosis, follow-up, and treatment of COVID-19 [5, 13, 17]. A comprehensive review on the role of imaging in the detection and management of COVID-19 is urgently needed. In this review, we searched Google Scholar, PubMed, and Web of Sciences using the keywords "coronavirus, or COVID-19, or 2019-nCoV, or pandemic" and "imaging" for alternative literature published before April 20, 2020. The search resulted in more than 3,000 publications in English. We then carefully selected the most appropriate articles about the imaging of COVID-19.

In section II, we will first introduce the imaging characteristics used in the detecting COVID-19. Then, the change of imaging characteristics during the follow-up and the treatment of COVID-19 patients is described in section III. Quantitative analysis could maximize the effectiveness of imaging, and the AI-based image analysis is conducted in section IV. Finally, we provide a thorough discussion of key findings in section V with a conclusion in section VI.

II. Imaging Modalities in Diagnosis of COVID-19

Medical imaging is a useful supplement to RT-PCR testing for the confirmation of COVID-19. Typical imaging characteristics, especially the CT characteristics, are found in COVID-19 patients. In the following subsections, we will introduce CT and other imaging modalities in confirmation of COVID-19.

A. The CT characteristics in confirmation of COVID-19

1) CT characteristics of typical COVID-19

Chest CT images of COVID-19 patients could be evaluated for the following characteristics [5, 13, 17-20] : (1) presence of GGO; (2) presence of consolidation, (3) laterality of GGO and consolidation; (4) number of lobes affected where either ground-glass or consolidative opacities are present; (5) degree

of involvement of each lung lobe, in addition to the overall extent of lung involvement measured, as measured by a "total severity score"; (6) presence of nodules; (7) presence of pleural effusion; (8) presence of thoracic lymphadenopathy (defined as lymph nodes size of ≥10 mm in a short-axis dimension); (9) airway abnormalities (including airway wall thickening, bronchiectasis, and endoluminal secretions); (10) axial distribution of disease (categorized as no axial distribution of the disease, central "peribronchovascular" predominant disease, or peripheral predominant disease); and (11) presence of underlying lung disease such as emphysema or fibrosis.

The above mentioned CT characteristics have got extensive attention from the clinicians [21]. The typical CT characteristics for four COVID-19 cases are shown in Figure 2. Table 1 shows several pieces of research about the CT characteristics in COVID-19.

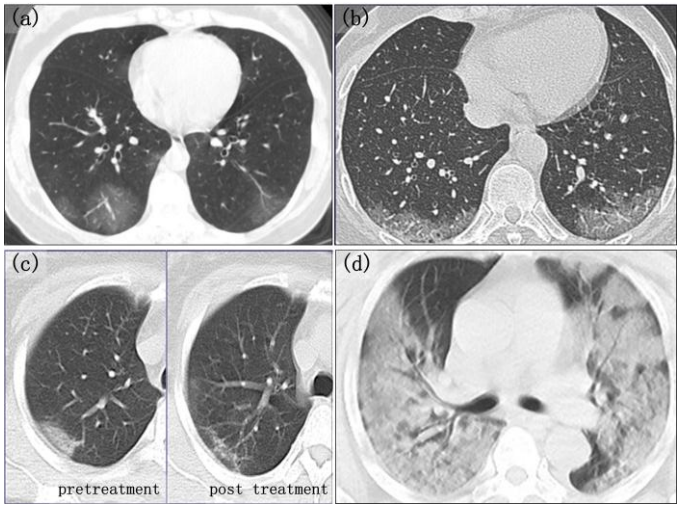

Figure 2. Four examples of COVID-19 patients from Beijing Youan Hospital. (a) Early stage patient: Female, 44 years old, fever for 3 days, body temperature 38.3℃, fatigue, cough. CT features: multiple pulmonary lobules involved, sub-pleural focal GGO accompanied by bronchial passage, thickened blood vessels, no mutual fusion or consolidation opacity. (b) Progression stage patient: Female, 56 years old, fever for 2 days, no cough, body temperature 37.3℃. CT features: multiple pulmonary lobules or involvement of lung segments in the advanced stage. Localized GGO accompanied by bronchi running under the pleura, thickened blood vessels, merged pulmonary lobule opacities, and local consolidation opacity. (c) Outcome stage patient: Female, 30 years old, fever and cough for 5 days. CT features: Multiple focal high-density opacities in both lung fields on the 5th day of onset (pretreatment); absorption improved on the 8th day of onset (post-treatment), showing streaky opacity only. (d) Severe (critical ill stage) patient: Male, 53 years old, fever for 3 days with dry cough, body temperature up to 39℃. CT features: The consolidation of the two lungs is known as "white lung", high-density opacity, occurs due to the alveoli being filled with a large number of phagocytes and neutrophil fragments, losing gas exchange capacity, and becoming consolidated.

GGO, which is defined as hazy increased lung attenuation with preservation of bronchial and vascular margins [26, 27], is the most common early finding of COVID-19 on chest CT. With respect to early manifestations of COVID-19 pneumonia, Han et al. [28] pointed out that early CT findings are multiple patchy pure GGO with or without consolidation involving multiple lobes, mainly in the peripheral zone, accompanied by a halo sign, vascular thickening, crazy paving pattern, or air bronchogram signs. Salehi et al. [29] performed a systematic review of imaging findings of COVID-19 and found that GGOs are prone to increase in number and size, and often progressively transform into multifocal consolidative opacities and septal thickening in the intermediate stage of the disease. The consolidation opacities will be absorbed, fibrotic stripes will form, and the number of lesions and involved lobes will decrease as a patient recovers [30]. Wu et al. [31] investigated 80 patients diagnosed with COVID-19 and found that 73% of the patients with clinical manifestations (e.g. cough and fever) also demonstrated multiple typical imaging features like interlobular septal thickening (ISH), GGO, and consolidation. Similar features and enlargement of vascular were also reported [22].

Table 1. Several studies of CT characteristics in COVID-19

Ref	Data Source	Number of patients	CT characteristics
Ai et al. [10]	Tongji Hospital, Wuhan, China	1014 suspected COVID-19 patients	**CT signs of suspected COVID-19:** Positive chest CT signs (888/1014, 88%); GGO (409/888, 46%); Consolidations (447/888, 50%); Bilateral chest CT signs (801/888, 90%). **CT signs of 413 RT-PCR negative suspected COVID-19:** Positive chest CT signs (308/413, 75%); Bilateral lung lesions (256/308, 83%); GGO; 41% (126/308, 41%); Consolidations 56% (172/308).
Zhao et al. [22]	Radiology Quality Control Center, Hunan, China	101 COVID-19 patients	**CT signs of COVID-19:** GGO (87/101, 86.1%); Mixed GGO and consolidation (65/101, 64.4%); Vascular enlargement in the lesion (71.3%); Traction bronchiectasis (53/101, 52.5%).
Bai et al. [23]	Seven hospitals from Hunan Providence, China; Rhode Island Hospital in Providence, RI, USA	219 COVID-19 patients and 205 patients with viral pneumonia	**CT signs COVID-19 *vs.* non-COVID-19:** Peripheral distribution (80% *vs.* 57%); GGO (91% *vs.* 68%); Fine reticular opacity (56% *vs.* 22%); Vascular thickening (58% *vs.* 22%); Reverse halo sign (11% *vs.*1%).
Zhu et al. [24]	First Affiliated Hospital of University of Science and Technology of China, Anhui, China	32 COVID-19 patients and 84 non-COVID-19 patients	**CT signs of COVID-19:** Pneumonia (30/32, 94%); Bilateral involvement (29/32, 91%); GGO (15/32, 47%); Spider web pattern (4/32, 13%).
Li et al. [25]	Second Affiliated Hospital of Chongqing Medical University, Chongqing, China	83 COVID-19 patients	**CT signs of COVID-19:** GGO (81/83, 97.6%); Linear opacities (54/83, 65.1%); Consolidation (53/83, 63.9%); Interlobular septal thickening (52/83, 62.7%); Crazy-paving pattern (30/83, 36.1%).

Besides GGO, bilateral patchy shadowing is one of the most common radiologic findings on chest CT [5, 16, 29]. Two studies have investigated the percentage of bilateral involvement in patients with COVID-19 [3, 17]. They studied

the degree of involvement in disease classification of the five lung lobes and found up to almost 100% bilateral involvement of them for patients with COVID-19. In a study of 41 patients in Wuhan, China, Huang et al. [32] claimed that abnormalities in chest CT images were detected among all patients, and most patients had bilateral involvement. The typical CT findings of ICU patients were bilateral multiple lobular and subsegmental areas of consolidation.

Consolidation and pulmonary fibrosis are also typical CT signs in the late stage of COVID-19. In a study involving 51 COVID-19 patients, Song et al. [33] concluded that lesions with consolidation could serve as either a marker of disease progression or of more severe disease. They also suggested that COVID-19 pneumonia should be highly suspected in patients with fever and/or cough, with GGO prominent lesions in the peripheral and posterior part of the lungs on CT images, combined with normal or decreased white blood cells, and an epidemiological history of exposure. Consolidation was found to be more common in pregnant women [26]. Sun et al. [34] found that the COVID-19 infection could increase the risk of pulmonary fibrosis, and they suggested that pulmonary fibrosis could become a critical complication in patients with COVID-19. Thus, it is important for clinicians to be alert to the occurrence of pulmonary fibrosis in COVID-19 patients.

Multiple lesions and crazy-paving pattern are also common in COVID-19 patients. Zhou et al. [35] found that, even on the initial CT scan, COVID-19 is more likely to manifest as multiple lesions rather than a single lesion. Moreover, in the early stage of the disease, the virus is more likely to invade the branches of the right inferior lobar bronchus and cause infection. The lesions showed a predominantly peripheral distribution, with the middle and lower zones and the posterior area of both lungs were significantly more involved. Li et al. [25] showed that 36% patients, especially the severe patients, have crazy-paving pattern in chest CT images, which could be a sign of poor condition.

2) CT characteristics in asymptomatic COVID-19

Screening of patients with asymptomatic or atypical presentation is an important aspect of controlling the spread of COVID-19. As CT plays an important role in the diagnosis of COVID-19, it is useful to explore the CT characteristics of asymptomatic and atypical patients. Hao et al. [36] found that, when the initial RT-PCR results of some patients were negative, chest CT showed typical radiographic findings, including GGO and/or mixed consolidation. Ai et al. [10] also reported the CT signs (bilateral lung lesions, GGO, and consolidations) of suspected COVID-19 patients with negative RT-PCR testing. Similarly, Fang et al. [37] reported that the CT signs of asymptomatic COVID-19 pneumonia included bifocal extra-zonal, bilateral and multifocal distribution.

However, not all asymptomatic patients have typical radiographic signs. Hu et al. [38] collected a total of 24 asymptomatic patients in China. These patients were confirmed to be positive for COVID-19 by testing the nucleic acid of pharyngeal swab samples. Of these 24 patients, 12 patients showed typical chest CT images, which included GGO shadows; 5 patients had fever, cough, fatigue and other symptoms during hospitalization, with chest CT images showing atypical radiographic signs (e.g., striped shadows in the lungs). The remaining 7 patients showed normal CT images in addition to having no clinical symptoms. In the statistical analysis of the patients' clinical characteristics, the authors found that 7 patients with normal CT findings and no symptoms were significantly younger than the other patients (median age: 14.0 years old, P = 0.012). That study also confirmed that asymptomatic patients were also contagious. Ling et al. [39] drew the same conclusions regarding the chest CT scans of asymptomatic patients: the authors retrospectively collected the data of 298 patients and found consistently negative CT images in 49 of the 295 patients. Of these 49 patients, 15 became positive after 3-6 days. The CT images of the other 34 patients remained negative for CT images, and it should be noted that 4 of them did not show any clinical symptoms or CT abnormalities. Therefore, not all asymptomatic patients have typical CT signs. The combination of chest CT imaging, RT-PCR, and close follow-up should be used to detect these asymptomatic COVID-19 patients.

3) Use of CT characteristics for discriminating COVID-19 pneumonia from other pneumonia

The use of CT findings for discriminating COVID-19 pneumonia from other pneumonia has attracted considerable attention. Upon reviewing coronavirus cases associated with severe acute respiratory syndrome (SARS) and Middle East respiratory syndrome (MERS), GGO and/or lung consolidation were typically characterized on chest CT, which is different from the characteristics of other viruses [40]. Similarly, the typical radiological features of COVID-19, multiple lobular GGO and subsegmental areas of consolidation are met more often [41]. Beyond that, most patients with COVID-19 pneumonia show bilateral involvement and multiple mottling, whereas the typical features of non-COVID-19 pneumonia are patchy shadows or density increasing shadows [41]. Compared to other pneumonia, patients with COVID-19 are more likely to exhibit CT abnormalities characterized by peripheral distribution, fine reticular opacity, vascular thickening, and reverse halo sign, but are less likely to have significant levels of central-peripheral distribution, pleural effusion, and lymphadenopathy [23]. As the disease progresses, there is rapid infiltration in lobes of COVID-19 patients as suggested by sequential CT scans from the same patient [24]. A part of late infection stage COVID-19 patients also exhibit spider web and crazy-paving patterns [14, 41].

B. Other imaging techniques in COVID-19 diagnosis

In addition to chest CT imaging, other imaging modalities are also used as complementary of chest CT in the diagnosis of COVID-19, including PET/CT, lung ultrasound, and magnetic resonance imaging (MRI). In the following sub-sections, a brief introduction of these imaging techniques is provided.

1) PET/CT

Positron emission tomography (PET) is a sensitive but invasive imaging method that, plays an important role in

evaluating inflammatory and infectious pulmonary diseases, monitoring disease progression and treatment effect, and improving patient management. Chu et al. [42] found that the SARS-CoV-2 infection caused inflammatory and significantly upregulated five inflammatory mediators, which indicates that the ^{18}F-FDG PET may be a potential imaging tool for COVID-19. Qin et al. [43] reported that lung lesions of patients with COVID-19 pneumonia were characterized by a high ^{18}F-FDG uptake, and the lymph node was involved, the disseminated disease was absent on ^{18}F-FDG PET/CT imaging. They suggest that ^{18}F-FDG PET/CT can play an auxiliary diagnostic role in COVID-19, especially in the early stage, when the differential diagnosis is difficult. In one case report, a high uptake of FDG was found in the lymph nodes and bone marrow by ^{18}F-FDG PET/CT evaluation [44]. Similarly, a high and significant ^{18}F-FDG uptake has been observed in patients with MERS-CoV infection [45]. In a letter to the editor, Deng et al. [46], suggested that FDG uptake may reflect non-specific inflammation or immune activation. FDG PET/CT can play an important role in identifying changes in uptake patterns and locations during viral exposure, and patients with higher FDG uptake in lesions may have a longer recovery period.

In contrast, another letter to the editor by Joob et al. [47], had a different view, staging that ^{18}F-FDG PET/CT is a more complex test than chest CT, and longer testing period for ^{18}F-FDG PET/CT examinations may increase risk of disease transmission. They conclude that further studies are needed to determine whether ^{18}F-FDG PET/CT is an appropriate testing modality for COVID-19, and this is currently not recommended for COVID-19 diagnosis.

2) Lung ultrasound

As a non-invasive, radiation-free, and portable imaging method, lung ultrasound (LUS) allows for the initial bedside screening of low-risk patients, diagnosis of suspected cases in the emergency room setting, prognostic stratification, and monitoring of the changes in pneumonia [48-50]. Peng et al. [51] reported that lung ultrasonography can provide results comparable with chest CT for evaluation of COVID-19 pneumonia. For severe or critical patients, especially those admitted to the ICU and requiring ventilation, LUS is necessary for patient management and monitoring the effectiveness of treatments. More importantly, the use of LUS can reduce the exposure risk between infected patients and health care workers, and discriminate between low-risk and higher-risk patients. Bunosenso et al. [52] reported a confirmed case that LUS showed an irregular pleural line with small subpleural consolidations, areas of white lung and thick, confluent and irregular vertical artifacts (B-lines). For pregnant women with suspected COVID-19, chest CT examination should be avoided as much as possible due to the high radiation dose risk to the fetus. As an alternative, Moro et al. [53] recommended that obstetricians and gynecologists to perform lung examination using LUS.

3) MRI

Magnetic resonance imaging (MRI) is a powerful radiation-free imaging technique for visualizing soft tissues. However, it is not commonly applied to COVID-19 diagnosis due to a relatively long scanning time and high cost compared to CT and LUS. Nonetheless, the non-invasive MRI may help in the evaluation of COVID-19 in children and pregnant women [54].

The infection of SARS-CoV-2 is mainly distributed in the lung, but three minimally invasive autopsies showed that the infection also involves in the damages of heart, vessels, liver, kidney, and other organs [55]. At the molecular level, Angiotensin-converting enzyme 2 (ACE2), the key host cellular receptor of SARS-CoV-2, has been identified in multiple organs. The study carried out by Chen et al. [56] confirmed that patients with basic heart failure disease showed increased ACE2 expression at both mRNA and protein levels and may have a higher risk of heart attack and critical ill condition. Similarly, cardiac MRI also showed cardiac involvements in patients with COVID-19, such as acute myopericarditis with systolic dysfunction [57]. At the RNA level, Zou et al. [58] identified other organs at risk like heart, esophagus, kidney, bladder, and ileum that are vulnerable to COVID-19 infection.

Due to excellent performance for visualizing structural and functional information of various soft organs, MRI could be used to study the vulnerability of different organs for a better understanding of the pathogenesis and mechanisms of COVID-19 infection. Meanwhile, similar to the study of Syrjala et al. [59], the ability of MRI, CT, and X-Ray can be evaluated, and in [60], the value and performance of LUS, X-Ray, CT, and MRI are compared for complicated pneumonia, many researches can be done for COVID-19 patients to not only compare different modalities or their combinations but also systematically study the organ damages and mechanisms of the disease.

III. The CT characteristics during the follow-up and treatment of COVID-19

Follow-up CT scans are often performed for patients with COVID-19 to assess the progression or improvement during the disease course. Moreover, quantitative follow-up can also improve the recognition of imaging characteristics with radiologists and assisted them in making a quick and accurate diagnosis. In this section, we focus on the CT manifestations in different stages of COVID-19; the quantitative CT metric changes with the advantage of COVID-19 progression are discussed; and the remission of lung lesions on CT images is depicted.

A. CT manifestations in different stages of COVID-19

Follow-up CT images reveal temporal changes in imaging characteristics for COVID-19 [26, 61-68]. By grouping COVID-19 patients based on disease courses, CT manifestations of lung lesions are analyzed based on different stages. Table 2 summarizes the related findings.

Table 2. Summary of the CT manifestations of COVID-19 in different stages

Ref.	Stage	CT characteristics	Number of COVID-19 patients
Bernheim et al. [61]	Early group (0-2 days)	No lung opacities or GGO	36
	Intermediate group (3-5 days)	GGO and consolidation	33
	Late group (6-12 days)	GGO, consolidation, linear opacities and crazy-paving pattern	25
Zhou et al. [35]	Early phase (≤7 days)	The frequency of GGO is significantly higher	40
	Advanced phase (8-14 days)	The frequency of GGO with a reticular pattern, vacuolar sign, fibrotic streaks, a subpleural line, a subpleural transparent line, air bronchogram, bronchus distortion, and pleural effusion is significantly higher	22
Pan et al. [69]	Stage-1 (0-4 days)	GGO with partial crazy-paving pattern and consolidation	24
	Stage-2 (5-8 days)	GGO extended to more lobes with more crazy-paving pattern and consolidation	17
	Stage-3 (9-13 days)	Consolidation as main manifestation with decreased GGO and crazy-paving pattern	21
	Stage-4 (⩾14 days)	Consolidation partially absorbed without any crazy-paving pattern	20
Wang et al. [70]	<0 days	Normal, or GGO and consolidation	10
	0-5 days	Predominant GGO with consolidation	79
	6-11 days	Predominant GGO with consolidation	85
	12-17 days	Predominant GGO with consolidation and increased mixed pattern	78
	18-23 days	Predominant GGO with mixed pattern	60
	⩾24 days	Predominant GGO with mixed pattern	54
Shi et al. [13]	Group 1 (<0 days)	Unilateral, multifocal GGO	15
	Group 2 (⩽7 days)	Bilateral and diffuse GGO	21
	Group 3 (8-14 days)	Predominant GGO with consolidation	30
	Group 4 (14-21 days)	Predominant GGO and reticular patterns	15
Chung et al. [63]	No change	No Changes	1
	Mild disease progression	Mild changes of opacities and density of consolidation	5
	Moderate disease progression	Increasing number of opacities and density of consolidation	2

The stages are mostly divided according to the time after the onset of clinical symptoms. In [35], the disease was roughly divided as the early phase (≤ 7 days) and advanced phase (8-14 days). In the early phase of disease, the frequency of GGO with a reticular pattern, vacuolar sign, fibrotic streaks, a subpleural line, a subpleural transparent line, air bronchogram, bronchus distortion, and pleural effusion is very high. Bernheim et al. [61] divided the patients into early group (0-2 days), intermediate group (3-5 days), and late group (6-12 days). In the early group, no lung opacities or slight GGO were observed among the patients. GGO and consolidation were frequently observed in patients in the intermediate group. In the late group, in addition to GGO and consolidation, linear opacities and crazy-paving pattern were also observed.

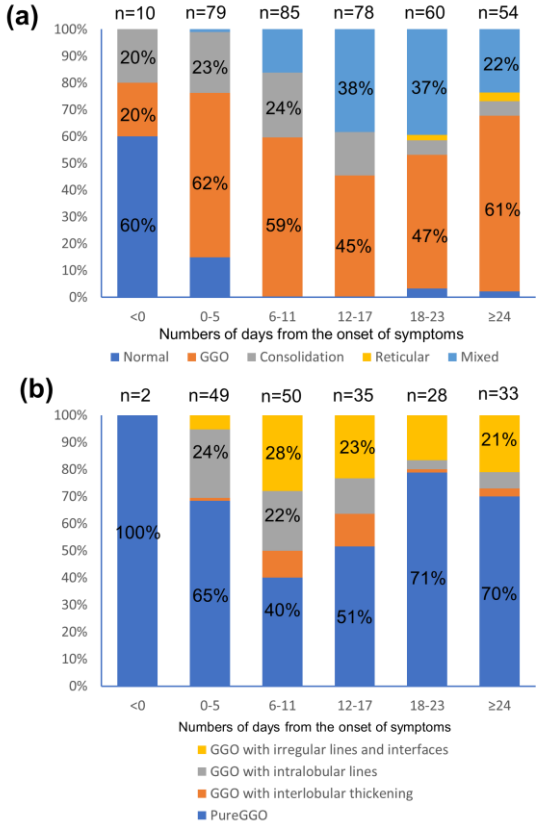

Figure 3. Temporal changes of main CT patterns and the subtypes of ground-glass opacity in [70]. (a) The distribution of CT manifestations of lung lesions; (b) the distribution of GGO subtype.

On the other hand, CT stages were divided into a more detailed description in the work of Pan [69] and Wang [70]. Pan et al. [69] divided patients into Stage-1 (0-4 days), Stage-2 (5-8 days), Stage-3 (9-13 days), and Stage-4 (≥14 days). Patients in Stage-1 had GGO with partial crazy-paving pattern and consolidation. In Stage-2, the GGO had extended to additional lobes, with increased crazy-paving pattern and consolidation. In Stage-3, consolidation became the main CT manifestation, and the GGO and crazy-paving patterns decreased. In Stage-4, the consolidation was partially absorbed without any crazy-paving pattern. Wang et al. [70] investigated temporal changes of chest CT characteristics, and divided the stages as < 0 days, 0-5 days, 6-11 days, 12-17 days, 18-23 days and ≥ 24 days (Figure 3). The lung lesions on CT images were predominantly manifested as GGO in most stages. In the earlier stages, each lung was divided into 3 zones: upper (above the carina), middle, and lower (below the inferior pulmonary vein) zones; each zone was evaluated for percentage of lung involvement on a scale of 0-4. They studied the median values of the total CT score and the number of zones involved as a function of time, and analyzed the temporal changes of the

main CT patterns (GGO and consolidation).

It can be drawn from previous studies that GGO was the main manifestation of COVID-19, especially in the early stages. With the progression of the disease, GGO gradually decreased, and consolidation became the increased pattern of lung lesions.

Many studies have reported an association between COVID-19 and the manifestation of clinical factors of RT-PCR results. Ai et al. enrolled 1014 suspected COVID-19 patients and reported that there was a correlation between COVID-19 and imaging manifestation of clinical factors [10]. In the initial group diagnosed as positive RT-PCR results, the authors reported that 60% of patients showed they had consistent CT features, including ground-glass opacity, consolidation, reticulation/thickened interlobular septa, nodules. Moreover, nearly all of the initial positive cases showed positive chest CT scans within a week. The findings revealed that chest CT detection is necessary to screen the suspected cases early. The authors also analyzed the CT images and serial RT-PCR assays, and found 60% to 93% of cases had the same manifestation of positive chest CT before the RT-PCR test [10]. With the COVID-19 patients gradually turning negative, the image manifestation also changed. CT images after recovery (RT-PCT negative) do not necessarily turn to negative at the same time, and the study suggests that CT examination is highly sensitive but absorption is relatively slow.

Li et al. [25] investigated the chest CT findings and clinical features associated with severe and critical COVID-19, and found that CT scores differed significantly between severe/critical and typical patients ($P < 0.001$).

Quantitative CT changes across the disease progression of COVID-19. As the disease progressed, the review conducted by Salehi et al. [29] suggests that progression is associated with both increased numbers and sizes of GGO combined with consolidative opacities and septal thickening, and severity can occur around 10 days after symptom onset. The work in [64] estimated the temporal change on chest CT for pregnant women with COVID-19 using a semi-quantitative scoring system. The work showed that pregnancy and childbirth did not aggravate the course of symptoms or CT characteristics of COVID-19, and they were mostly mild type, presenting with clinical features and CT imaging progression pattern similar to those of non-pregnant women. Pan et al. in [69] recorded the changes in CT scans of 21 RT-PCR confirmed COVID-19 patients from the initial diagnosis to recovery. The results showed that about 91% of patients attached the greatest severity (with the highest score obtained) in the peak stage (9-13 days after onset). In conclusion, the authors suggested that the greatest severity was attached approximately 10 days after the initial symptoms. These works showed that follow-up CT characteristic analyses in a short time were feasible.

B. Remission of lung lesions on CT images

Several studies have described changes in CT images during the recovery process in COVID-19 infection after treatment. In a report by Liu et al. [71], the size of lung lesions had decreased by more than half in 67% of patients at one week after receiving antiviral and supportive treatment; this manifested on CT images as remarkable absorption and residual interstitial abnormalities with persisting septal lines. In a case report by Fang et al. [72], the extent and density of the patient's lung lesions had significantly decreased after 3 days of antiviral and anti-inflammatory treatment. Thus, it appears that detecting lung recovery using CT scans is feasible.

IV. AI-BASED IMAGE ANALYSIS FOR COVID-19

Due to the rapid spread of COVID-19, medical resources became insufficient in many regions. Using AI to assist the disease management of COVID-19 is important. Manual diagnosis in CT scanning requires a lot of manual labor and consumes a lot of time. In order to reduce the workloads of radiologists, computer-aided diagnostic tools have been developed based on deep learning or machine learning technology. These tools have shown the potentials to increase diagnostic efficiency and reduce the pressure of radiologists (Table 3).

Table 3. COVID-19 analysis with CT images and AI.

Ref	Number of patients	Task	Methods	Validation	Performance
Chen [73]	51 COVID-19, 82 others	COVID-19 diagnosis	UNet++	Random patient-level	ACC= 0.95
Fang [74]	46 COVID-19, 29 other pneumonia	COVID-19 diagnosis	Radiomic feature, consensus clustering	Random Patient-level	AUC= 0.826
Wang [75]	44 COVID-19 55 viral pneumonia	COVID-19 diagnosis	Manual, ResNet34, Decision tree	Random ROI level	AUC= 0.78
Xu [76]	110 COVID-19, 224 viral pneumonia, 175 healthy	COVID-19 diagnosis	3D CNN, 3DResNet	Random Patient-level	ACC= 0.86
Jin [77]	723 COVID-19, 413 others	COVID-19 diagnosis	UNet++, ResNet50	Random Patient-level	SEN= 0.97 SPE= 0.92
Song [78]	88 COVID-19, 100 bacterial pneumonia	COVID-19 diagnosis	OpenCV, DRE-Net	Random Patient-level	AUC= 0.95
Jin [79]	496 COVID-19, 260 others	COVID-19 diagnosis	2D CNN	Random Patient-level	AUC= 0.98
Zheng	313 COIVD-19,	COVID-19 diagnosis	UNet, 3DResN	Random Patient-le	AUC= 0.98

[80]	229 others		et	vel	
Li [81]	468 COVID-19, 1,551 CAP, 1,303 others	COVID-19 diagnosis	UNet, ResNet50	Random Patient-level	AUC= 0.96
Shi [82]	1,658 COVID-19, 1,027 CAP	COVID-19 diagnosis	VBNet, Hand-crafted feature, Random forest	Random Patient-level	ACC= 0.88
Wang [83]	4,106 lung cancer, 924 COVID-19, 342 other pneumonia	COVID-19 diagnosis, prognosis	FPN, DenseNet	External Patient-level	AUC = 0.87 AUC = 0.88
Shi [84]	151 non-severe, 45 severe	Severity diagnosis of COVID-19	V-Net, LASSO, Logistic regression	Random Patient-level	AUC= 0.89

Note: ACC, AUC, SEN and SPE represent accuracy, area under the receiver operator characteristics curve, sensitivity, and specificity.

Many recently published studies indicated that COVID-19 usually demonstrates GGO or lesions in CT images [13, 27]. Consequently, finding abnormal areas such as GGO or lesions in CT images is important for the diagnosis of COVID-19 for radiologists. Automatically detecting GGO or nodules in CT images can help reduce human effort. Chen et al. [73] used UNet++ [85] to extract abnormal lung areas in CT images. UNet++ is a modification of the UNet model, which is originally designed for biomedical image segmentation. Given a CT image slice, the UNet++ model can segment the areas with lesions. Afterwards, the bounding box of the segmented lesion is generated. In their study, 2D CT image slices of 106 patients (51 with COVID-19, and 55 with other diseases) were randomly divided into training and internal validation sets at the image slice-level. To predict by case, a logic linking the prediction results of consecutive images was added. CT images with the above prediction results were divided into four quadrants, and results would be output only when three consecutive images were predicted to have lesions in the same quadrant. In the internal validation set, the model correctly diagnosed the patients with a per-patient sensitivity of 100%, specificity of 93.55%, and accuracy of 95.24%. A per-image sensitivity of 94.34%, specificity of 99.16%, and accuracy of 98.85% were detected. Notably, this study used a prospective set including 27 patients for further validation, and the model achieved comparable performance to that of an expert radiologist. With the assistance of the model, the reading time of radiologists was greatly decreased by 65%.

Instead of only detecting abnormal or infectious areas, an AI model that can directly diagnose COVID-19 is more convenient to use. Fang el al. [74] used radiomics analysis method to diagnose COVID-19. In their study, 77 radiomic features were extracted from manually delineated ROI, and unsupervised consensus clustering was used to select important features that showed a relationship with COVID-19. Finally, support vector machine (SVM) classifier was used to classify COVID-19 using the selected features. In this study, 75 patients (46 COVID-19, 29 other pneumonia) from a single center were collected, and 25 patients were randomly selected as the testing set. The radiomic model achieved AUC of 0.826 in the testing center. Wang el al. [75] designed a deep-learning model to screen COVID-19 from typical viral pneumonia. Radiologists first annotated the infectious area as the region of interest (ROI). Afterwards, a modified ResNet34 was used to extract the deep learning feature, and a combination of decision tree and AdaBoost was used to classify COVID-19 and typical viral pneumonia. In the 99 patients (44 COVID-19 and 55 typical viral pneumonia patients), the model achieved an accuracy of 73.1% at the ROI-level. Since human annotated ROIs can be affected by different users and are time-consuming, Xu et al. [76] proposed a deep-learning model to automatically detect infectious areas in CT images, and then used 3DResNet to identify whether the infectious areas were COVID-19. The candidate infectious regions were first segmented out using a 3D deep-learning model from a pulmonary CT image set. These separated images were then categorized into COVID-19, influenza-A viral pneumonia or healthy groups, together with the corresponding confidence scores using a location-attention classification model. Finally, the infection type and total confidence score of this CT case were calculated with noisy or Bayesian function. In the retrospective data set (110 with COVID-19, 224 with influenza-A viral pneumonia, 175 CT samples from healthy people), 85.4% CT samples were randomly selected for training, and the rest 14.6% CT samples were used for testing. The deep-learning model achieved an accuracy of 86.7 % in the testing set. Similarly, Jin et al. [77] developed an AI-system for COVID-19 lesion segmentation and classification. This model included three steps. First, lung regions were extracted using 3D-UNet; then, specific lesions were segmented in the lung regions; finally, a CNN-based classifier divided the lesions as being positive or negative. This system was trained with 1,136 training cases (723 positives for COVID-19) from 5 hospitals. It achieved a sensitivity of 0.974 and specificity of 0.922 in the testing set, which satisfied the requirement of clinical application.

Unlike detecting infectious regions for classification, Song et al. [78] extracted the whole lung area for classification. First, they extracted the main regions of the lungs and filled the blank of lung segmentation with the lung itself to avoid noise caused by different lung contours. Then, they designed a Details Relation Extraction neural network (DRE-Net) to extract the top-K details in the CT images and obtain image-level predictions. Finally, the image-level predictions were aggregated to achieve patient-level diagnoses. Eighty-eight COVID-19 and 100 bacterial pneumonia patients were used to train and validate the performance of the deep-learning model. In the testing set, the model achieved an AUC of 0.95 and sensitivity of 0.96. In [79], Jin et al. built a deep-learning-based diagnosis method to accelerate the speed of COVID-19 diagnosis. This deep-learning model was trained using only 312 cases' images. However, it achieved comparable performance with experienced radiologists. Among 1,255 independent

testing cases, the proposed deep-learning model achieved an accuracy of 94.98%, an AUC of 97.91%, a sensitivity of 94.06% and a specificity of 95.47%. Another reader study was conducted and only one radiologist's performance was slightly better than this deep-learning model while this model could finish the diagnosis in a much shorter time.

Infectious areas can be distributed in many locations in the lungs, and automatic infectious area detection may not guarantee very high precision. Consequently, using the whole lung for classification is more convenient in practice. Zheng et al. [80] used UNet [86] to segment the lung area automatically, and then used 3DResNet for classification. In their data set including 313 COVID-19 and 229 patients without COVID-19, patients were divided into a training set and a testing set according to their CT scanning time. Patients who performed CT scanning before Jan. 23, 2020 were used for training, and patients who performed CT scanning after Jan. 23, 2020 were used for testing. In the testing set including 131 patients, the deep-learning model achieved an AUC of 0.976. Similarly, Gozes et al. [87] used 157 patients from both China and the US as the testing set. The deep-learning model achieved an AUC of 0.996.

Due to the emergence of COVID-19, a big data set for training and validating AI models is necessary. In [81], 3,506 patients (468 with COVID-19, 1,551 with Community Acquired Pneumonia (CAP), and 1,303 with non-pneumonia) were used to train and test the deep-learning model. Similar to other studies [78, 87], Li et al. first used U-net to extract the whole lung region as an ROI. Afterwards, 2D RestNet50 was used for classifying COVID-19. Since each CT scanning includes multiple 2D image slices, the features in the last layer of ResNet50 were max pooled and combined for prediction. In the testing set including 1/9 randomly selected patients, the deep-learning model achieved an AUC of 0.96 in classifying COVID-19 from CAP and other pneumonia. Shi et al. [82] included 1658 patients with COVID-19 and 1,027 patients with CAP for classification. They first used VBNet [88] to segment infected areas, bilateral lungs, 5 lung lobes, and 18 lung pulmonary areas. Then, hand-crafted features such as infection size, location specific features and radiomic features were extracted, and least absolute shrinkage and selection operator (LASSO) was used for feature selection. Random forest was used for classification. In the five-fold validation, the method achieved sensitivity of 0.907, specificity of 0.833, and accuracy of 0.879. In another study, Wang et al. [83] proposed a fully automatic deep-learning system for COVID-19 classification and prognostic analysis. In their study, an FPN network [89] with a DenseNet121 [90] backbone was used to segment lung areas automatically. Afterwards, a network using a DenseNet structure was built to classify COVID-19 and other pneumonia. Instead of using transfer learning from natural images, they collected 4106 patients with EGFR gene mutation status to pre-train the model [91]. Afterwards, 924 patients with COVID-19 and 342 patients with other pneumonia were used to train and validate the model. Notably, they used patients from 2 provinces in China (Heilongjiang and Anhui) for external validation. In the two independent validation sets, the deep-learning model achieved an AUC of 0.87 and 0.88. In addition, the prognostic value of the deep-learning model was explored. Features from the fully connected layer of the deep-learning model were used for prognostic feature selection. Afterwards, the Cox proportional hazard model [92] was used to predict the hospital-stay time of patients with COVID-19. In another 2 external validation sets from Huangshi city and Beijing, the Cox model could stratify patients into high-risk and low-risk groups with different hospital-stay time (p<0.05, Kaplan-Meier analysis).

Except for diagnosing COVID-19, AI also shows good performance in predicting the severity of COVID-19. Shi et al. [84] proposed a deep-learning-based quantitative assessment method to predict the severity of COVID-19 (severe vs. non-severe). The deep learning method calculated two indices named mass of infection (MOI) and the percentage of infection (POI), which had higher values in the severe group than the non-severe group of patients. Then, the LASSO logistic regression model combined POI and MOI with clinical features such as age, lactate dehydrogenase (LDH), C-reactive protein (CRP) and CD4+ T cell counts to classify the patients as severe patients or non-severe patients. The AUC in the testing dataset achieved 0.89, which was significantly higher than the baseline pneumonia severity index. Current studies indicated that AI shows good performance in quickly diagnosing COVID-19. With the assistance of AI, clinicians can be separated from patients to avoid infection. On the other hand, CT image is easy to acquire. Using AI and CT images to diagnose COVID-19 does not add additional cost.

V. Discussion

The COVID-19 pandemic has affected over two million patients and rapidly become a major global health threat. Imaging techniques, in particular CT, play a critical role in diagnosis and monitoring COVID-19 pneumonia. In the majority of current studies, CT remains the primary tool for assessing lung lesions in COVID-19 cases, and changes in the severity of lung lesions. With the progression of CIVID-19, different degrees of lung lesions can be observed by multiple CT scans.

The most common CT manifestation of COVID-19 is GGO, followed by consolidation. With the advance of disease, a decrease in GGO and an increase in consolidation can be observed. In addition, pure GGO also gradually becomes more diversified CT features including crazy-paving pattern, reticular pattern, vacuolar sign, fibrotic streaks, a subpleural line, a subpleural transparent line, air bronchogram, and bronchus distortion in this process. However, the clinical manifestations can vary between patients, which helps to explain some discrepancies between different studies. Changes in lung lesions are closely related to the disease progression of COVID-19. For example, patients with rapid disease progression also exhibit a rapid enlargement of lung lesions on CT imaging within 24-48 hours. The response to treatment also varies between patients. In most patients with mild disease, the lung lesions are absorbed after receiving treatment. However, lung lesions of patients with severe or critical disease may be

irreversible. Current studies on the follow-up CT scans for COVID-19 are still dealing with a small number of samples. Additional research, ideally multi-center data with large sample sizes, is needed to provide further insights into the evolution of lung lesions during and after an infection caused by COVID-19.

In the clinical diagnosis of COVID-19, chest CT can supplement RT-PCR testing and compensate for its relatively poor sensitivity. Ai et al. [10] compared the diagnostic value and consistency of chest CT scans and RT-PCR results from the swab samples of 1,014 patients in the epidemic area of China, all of whom had undergone both chest CT and RT-PCR testing. They demonstrated a higher sensitivity of chest CT than of RT-PCR for the diagnosis of COVID-19. With the RT-PCR results as a reference, the sensitivity, specificity, and accuracy of chest CT in determining SARS-CoV-2 infection were 97%, 25%, and 68%, respectively. The PPV and NPV were 65% and 83%, respectively. Moreover, Fu et al. [11] analyzed the data of 52 patients with COVID-19 who had been discharged and found heterogeneity between chest CT findings and RT-PCR results, especially in some of the recovered patients with negative RT-PCR results. Some patients with COVID-19 will have negative nucleic acid test results, and yet they can still exhibit inflammatory changes that are visible on chest CT images [12]. Thus, chest CT combined with epidemiological history and laboratory tests is useful for detecting COVID-19 and evaluating progression and treatment effects [93]. However, it is important to note that Guan et al. [5] reported that many patients do not exhibit abnormal radiologic findings, and such patients should not be overlooked in the screening and diagnosis of COVID-19. For asymptomatic patients, especially for those who showed normal CT findings without any clinical symptoms, the combination of chest CT imaging, RT-PCR, epidemiological history, and close follow-up is highly recommended to confirm these asymptomatic COVID-19 patients.

Due to the emergent nature of COVID-19, the medical resources in many parts of the world are insufficient. Quickly diagnosing COVID-19 and predicting individualized prognosis are important for the management of COVID-19. Recent studies have reported promising results of the use of AI combined with CT imaging, which can assist in the rapid diagnosis of COVID-19 and prognostic predictions. As CT images exhibit several prognostic and diagnostic characteristics of COVID-19, the rapid and precise quantification of these characteristics using AI has garnered considerable attention. Three types of AI strategies have been reported: 1) use AI to detect lesions to assist fast screening of COVID-19 for clinicians; 2) use AI to diagnose COVID-19 using partial or whole lung in CT images; 3) use AI to predict other clinical outcomes of COVID-19 (e.g., severity of COVID-19). Among the studies using deep learning for diagnosing COVID-19, UNet and its modifications were often used for segmenting lung or lesions from CT images, and ResNet (2D or 3D) were often used for classification. Compared with studies using segmented lung lesions for classification, using the whole lung for analysis achieved similar results, which may suggest that segmenting or detecting lung lesions for analysis may not be necessary. Since lesion segmentation is more difficult than lung segmentation, and multiple lesions or infectious areas can exist in lung, using the whole lung for analysis is more reasonable and convenient.

Despite promising results in recent studies [74, 84], many AI models were tested in small datasets. The studies using small dataset (e.g., <300 patients) often showed high AUC or accuracy. However, in several studies with larger dataset (> 1000 patients) [13, 83], the performance drops. Consequently, the very high accuracy of AI models in small dataset may be caused by overfitting. The larger scale studies with lower accuracy may reflect the real ability of what AI could do in diagnosing COVID-19. On the other hand, very few studies used independent and external validation dataset to evaluate the generalization ability of deep learning models. In the future study, large external validation dataset should be used. Due to the limited training data of COVID-19, transfer learning using chest CT images should be a good strategy. In [83], the CNN model was first trained using lung cancer dataset including 4106 patients, and finally achieved good performance in diagnosing COVID-19. Many transfer learning models in current studies used ResNet that was pre-trained in ImageNet dataset. Using chest CT image for transfer learning may be a better choice, such as using the LIDC-IDRI dataset for pre-training. In addition, many of the previous studies on AI have focused on the rapid diagnosis of COVID-19. However, the prognostic analysis of COVID-19 is essential to the management of COVID-19, and combined AI and CT imaging can play an important role in treatment and management. For example, AI and CT can be used to identify patients with a high risk of progressing to severe disease or even of dying; it can also be used to evaluate or predict the response of specific therapies.

Although CT is the primary tool for screening and evaluating disease severity in patients with COVID-19, other clinical imaging methods, such as PET, MRI, and ultrasound have also added value by identifying specific imaging features that can be used for the diagnosis of pneumonia. These clinical imaging tools can be used as a complement to chest CT in the examination of COVID-19 pneumonia, especially for patients with comorbidities. MRI plays a key role in pediatric examinations and evaluating cardiac involvement of COVID-19. PET can be used for reviewing inflammatory and infectious pulmonary diseases. In addition, PET is a promising imaging tool in monitoring disease progression and treatment effect, and improving patient management. In particular, LUS has shown potential in the examination and management of COVID-19. It is especially suitable for screening pregnant women and children, especially for patients admitted to ICU, due to being radiation-free, low-cost, and portable. However, LUS results may vary with different operators. Guidelines for LUS examinations of COVID-19 pneumonia should be developed as soon as possible.

COVID-19 is highly transmissible, highly pathogenic and deadly, especially in the elderly and patients with underlying diseases. COVID-19 has highly occult clinical symptoms.

Individual differences in clinical symptoms and laboratory indicators (C-reactive protein, lymphocytes) of patients increase in the acute phase, and decrease or return to normal in the recovery phase. According to one literature report [10], about 97% of COVID-19 patients tested positive for CT, which plays an important role in the specific environment and high-risk groups. It provided important evidence-based proof for clinical practice. However, we must admit that nucleic acid test results are still the gold standard of clinical diagnosis. It is suggested that epidemiology, nucleic acid detection results, CT image features, clinical symptoms and laboratory indicators should be taken into consideration to make a comprehensive and objective assessment, so as to avoid a missed diagnosis or misdiagnosis and effectively improve the clinical effects.

VI. Conclusion

In summary, various imaging technologies can play important roles in the management of COVID-19. Nucleic acid testing remains the gold standard of clinical diagnosis. However, various imaging characteristics, especially those of CT scans, can reflect lung area changes, bronchial changes, and pleural changes. Typical CT signs of COVID-19 include GGO, consolidation, vascular enlargement, and pleural thickening. The majority of cases show bilateral involvement and multiple mottling. The joint use of these imaging biomarkers and RT-PCR testing can improve COVID-19 screening and diagnosis. Moreover, 97% of COVID-19 patients show positive CT manifestations [10]. The use of chest CT scans can counteract the limitations of epidemiological tracing and the low sensitivity of nucleic acid detection, thus improving the accuracy and speed of diagnosis and patient management. The findings of this review suggest that COVID-19 diagnosis should be based on epidemiological history, nucleic acid detection, CT imaging, clinical symptoms and signs, and laboratory findings. The combined use of AI and CT imaging can offset limitations in medical resources, as well as support the rapid diagnosis and prognostic prediction of COVID-19. Future studies of combined AI and CT imaging, using largely and externally validated data sets, are needed.

Though the follow-up CT studies for COVID-19 is still limited for now, common changing pattern of lung lesions can still be observed, which including GGO in the relatively early stages and increased consolidation with the advance of disease. In process of remission, the recovery patterns are mostly manifested as lesion absorbing. CT scans have proved as an efficient clinical tool in assessing the progression and remission of lung lesions in COVID-19 infection. Multi-center studies with large sample-size are still needed to ascertain the current findings.

References

[1] J. F. Chan *et al.*, "A familial cluster of pneumonia associated with the 2019 novel coronavirus indicating person-to-person transmission: a study of a family cluster," *Lancet,* vol. 395, no. 10223, pp. 514-523, Feb 15 2020, doi: 10.1016/S0140-6736(20)30154-9.

[2] N. Zhu *et al.*, "A Novel Coronavirus from Patients with Pneumonia in China, 2019," *New England Journal of Medicine,* vol. 382, no. 8, pp. 727-733, 2020, doi: 10.1056/NEJMoa2001017.

[3] N. Chen *et al.*, "Epidemiological and clinical characteristics of 99 cases of 2019 novel coronavirus pneumonia in Wuhan, China: a descriptive study," *The Lancet,* vol. 395, no. 10223, pp. 507-513, 2020.

[4] X. Yang, Y. Yu, and J. Xu, "Clinical course and outcomes of critically ill patients with SARS-CoV-2 pneumonia in Wuhan, China: a single-centred, retrospective, observational study (vol 17, pg 534, 2020)," *Lancet Respiratory Medicine,* vol. 8, no. 4, pp. E26-E26, Apr 2020. [Online]. Available: <Go to ISI>://WOS:000522760200013.

[5] W.-j. Guan *et al.*, "Clinical Characteristics of Coronavirus Disease 2019 in China," *New England Journal of Medicine,* 2020, doi: 10.1056/NEJMoa2002032.

[6] Z. Wu and J. M. McGoogan, "Characteristics of and Important Lessons From the Coronavirus Disease 2019 (COVID-19) Outbreak in China: Summary of a Report of 72 314 Cases From the Chinese Center for Disease Control and Prevention," *JAMA,* vol. 323, no. 13, pp. 1239-1242, 2020, doi: 10.1001/jama.2020.2648.

[7] M. D. Hope, C. A. Raptis, and T. S. Henry, "Chest Computed Tomography for Detection of Coronavirus Disease 2019 (COVID-19): Don't Rush the Science," *Annals of Internal Medicine,* 2020, doi: 10.7326/M20-1382.

[8] W. H. Organization, "Clinical management of severe acute respiratory infection when Novel coronavirus (2019-nCoV) infection is suspected: Interim Guidance."

[9] *National Health Commission of the People's Republic of China, Diagnosis and treatment protocol for COVID-19 (trial version 7)*. [Online] Available: http://en.nhc.gov.cn/2020-03/29/c_78469.htm

[10] T. Ai *et al.*, "Correlation of chest CT and RT-PCR testing in coronavirus disease 2019 (COVID-19) in China: a report of 1014 cases," *Radiology,* p. 200642, 2020.

[11] H. Fu *et al.*, "Association between Clinical, Laboratory and CT Characteristics and RT-PCR Results in the Follow-up of COVID-19 patients," *medRxiv,* 2020.

[12] X. Xie, Z. Zhong, W. Zhao, C. Zheng, F. Wang, and J. Liu, "Chest CT for typical 2019-nCoV pneumonia: relationship to negative RT-PCR testing," *Radiology,* p. 200343, 2020.

[13] H. Shi *et al.*, "Radiological findings from 81 patients with COVID-19 pneumonia in Wuhan, China: a descriptive study," *The Lancet. Infectious diseases,* 2020-Feb-24 2020, doi: 10.1016/s1473-3099(20)30086-4.

[14] J. P. Kanne, "Chest CT Findings in 2019 Novel Coronavirus (2019-nCoV) Infections from Wuhan, China: Key Points for the Radiologist," *Radiology,* vol. 295, no. 1, pp. 16-17, Apr 2020, doi: 10.1148/radiol.2020200241.

[15] Z. Ye, Y. Zhang, Y. Wang, Z. Huang, and B. Song, "Chest CT manifestations of new coronavirus disease 2019 (COVID-19): a pictorial review," *European Radiology,* 2020/03/19 2020, doi: 10.1007/s00330-020-06801-0.

[16] A. J. Rodriguez-Morales *et al.*, "Clinical, laboratory and imaging features of COVID-19: A systematic review and meta-analysis," *Travel Medicine and Infectious Disease,* p. 101623, 2020/03/13/ 2020, doi: https://doi.org/10.1016/j.tmaid.2020.101623.

[17] D. Wang *et al.*, "Clinical characteristics of 138 hospitalized patients with 2019 novel coronavirus–infected pneumonia in Wuhan, China," *Jama,* 2020.

[18] A. Bernheim *et al.*, "Chest CT findings in coronavirus disease-19 (COVID-19): relationship to duration of infection," *Radiology,* p. 200463, 2020.

[19] L. L. Zhang, D. N. C. Wang, Q. H. Huang, and X. D. Wang, "Significance of clinical phenomes of patients with COVID-19 infection: A learning from 3795 patients in 80 reports," *Clinical and Translational Medicine*, doi: 10.1002/ctm2.17.

[20] J. Liu, H. Yu, and S. Zhang, "The indispensable role of chest CT in the detection of coronavirus disease 2019 (COVID-19)," (in eng), *Eur J Nucl Med Mol Imaging,* pp. 1-2, 2020, doi: 10.1007/s00259-020-04795-x.

[21] Y.-H. Jin *et al.*, "A rapid advice guideline for the diagnosis and treatment of 2019 novel coronavirus (2019-nCoV) infected pneumonia (standard version)," *Military Medical Research,* vol. 7, no. 1, p. 4, 2020.

[22] W. Zhao, Z. Zhong, X. Xie, Q. Yu, and J. Liu, "Relation between chest CT findings and clinical conditions of coronavirus disease (COVID-19) pneumonia: a multicenter study," *American Journal of Roentgenology,* pp. 1-6, 2020.

[23] H. X. Bai *et al.*, "Performance of radiologists in differentiating COVID-19 from viral pneumonia on chest CT," *Radiology,* p. 200823, 2020.

[24] W. Zhu, K. Xie, H. Lu, L. Xu, S. Zhou, and S. Fang, "Initial clinical features of suspected Coronavirus Disease 2019 in two emergency departments outside of Hubei, China," *Journal of Medical Virology,* 2020.

[25] K. Li *et al.*, "The clinical and chest CT features associated with severe and critical COVID-19 pneumonia," *Investigative radiology,* 2020.

[26] H. Liu, F. Liu, J. Li, T. Zhang, D. Wang, and W. Lan, "Clinical and CT Imaging Features of the COVID-19 Pneumonia: Focus on Pregnant Women and Children," *The Journal of infection,* 2020-Mar-11 2020, doi: 10.1016/j.jinf.2020.03.007.

[27] M. Chung *et al.*, "CT imaging features of 2019 novel coronavirus (2019-nCoV)," *Radiology,* p. 200230, 2020.

[28] R. Han, L. Huang, H. Jiang, J. Dong, H. Peng, and D. Zhang, "Early Clinical and CT Manifestations of Coronavirus Disease 2019 (COVID-19) Pneumonia," *American Journal of Roentgenology,* pp. 1-6, 2020.

[29] S. Salehi, A. Abedi, S. Balakrishnan, and A. Gholamrezanezhad, "Coronavirus Disease 2019 (COVID-19): A Systematic Review of Imaging Findings in 919 Patients," (in eng), *AJR. American journal of roentgenology,* pp. 1-7, Mar 14 2020, doi: 10.2214/ajr.20.23034.

[30] Y. H. Xu *et al.*, "Clinical and computed tomographic imaging features of novel coronavirus pneumonia caused by SARS-CoV-2," *Journal of Infection,* vol. 80, no. 4, pp. 394-400, Apr 2020, doi: 10.1016/j.jinf.2020.02.017.

[31] J. Wu *et al.*, "Chest CT findings in patients with corona virus disease 2019 and its relationship with clinical features," *Investigative Radiology,* vol. 670, 2020.

[32] C. Huang *et al.*, "Clinical features of patients infected with 2019 novel coronavirus in Wuhan, China," *The Lancet,* vol. 395, no. 10223, pp. 497-506, 2020.

[33] F. Song *et al.*, "Emerging 2019 novel coronavirus (2019-nCoV) pneumonia," *Radiology,* p. 200274, 2020.

[34] P. Sun, S. Qie, Z. Liu, J. Ren, K. Li, and J. Xi, "Clinical characteristics of 50466 hospitalized patients with 2019-nCoV infection," *Journal of medical virology,* 2020.

[35] S. Zhou, Y. Wang, T. Zhu, and L. Xia, "CT Features of Coronavirus Disease 2019 (COVID-19) Pneumonia in 62 Patients in Wuhan, China," *American Journal of Roentgenology,* pp. 1-8, 2020.

[36] W. Hao and M. Li, "Clinical diagnostic value of CT imaging in COVID-19 with multiple negative RT-PCR testing," *Travel medicine and infectious disease,* p. 101627, 2020.

[37] Y. Fang *et al.*, "Sensitivity of Chest CT for COVID-19: Comparison to RT-PCR," *Radiology,* p. 200432, 2020, doi: 10.1148/radiol.2020200432.

[38] Z. Hu *et al.*, "Clinical characteristics of 24 asymptomatic infections with COVID-19 screened among close contacts in Nanjing, China," *Science China Life Sciences,* pp. 1-6, 2020.

[39] Z. Ling *et al.*, "Asymptomatic SARS-CoV-2 infected patients with persistent negative CT findings," *European Journal of Radiology,* 2020.

[40] L. A. Marinari, M. A. Danny, and W. T. Miller, "Sporadic coronavirus lower respiratory tract infection in adults: chest CT imaging features and comparison with other viruses," *European Respiratory Journal,* vol. 54, Sep 2019, doi: 10.1183/13993003.congress-2019.PA4547.

[41] D. Zhao *et al.*, "A comparative study on the clinical features of COVID-19 pneumonia to other pneumonias," *Clinical Infectious Diseases,* 2020.

[42] H. Chu *et al.*, "Comparative replication and immune activation profiles of SARS-CoV-2 and SARS-CoV in human lungs: an ex vivo study with implications for the pathogenesis of COVID-19," *Clinical Infectious Diseases,* 2020, doi: 10.1093/cid/ciaa410.

[43] C. Qin, F. Liu, T.-C. Yen, and X. Lan, "F-18-FDG PET/CT findings of COVID-19: a series of four highly suspected cases," *Eur J Nucl Med Mol Imaging,* 2020, doi: 10.1007/s00259-020-04734-w.

[44] S. Zou and X. Zhu, "FDG PET/CT of COVID-19," *Radiology,* p. 200770, Mar 6 2020, doi: 10.1148/radiol.2020200770.

[45] K. M. Das, E. Y. Lee, R. D. Langer, and S. G. Larsson, "Middle east respiratory syndrome coronavirus:

what does a radiologist need to know?," *American Journal of Roentgenology,* vol. 206, no. 6, pp. 1193-1201, 2016.

[46] Y. Deng, L. Lei, Y. Chen, and W. Zhang, "The potential added value of FDG PET/CT for COVID-19 pneumonia," (in eng), *Eur J Nucl Med Mol Imaging,* pp. 1-2, Mar 21 2020, doi: 10.1007/s00259-020-04767-1.

[47] B. Joob and V. Wiwanitkit, "18F-FDG PET/CT and COVID-19," *Eur J Nucl Med Mol Imaging,* pp. 1-1, 2020.

[48] G. Soldati *et al.*, "Is there a role for lung ultrasound during the COVID-19 pandemic?," *Journal of ultrasound in medicine : official journal of the American Institute of Ultrasound in Medicine,* 2020-Mar-20 2020, doi: 10.1002/jum.15284.

[49] E. Poggiali *et al.*, "Can Lung US Help Critical Care Clinicians in the Early Diagnosis of Novel Coronavirus (COVID-19) Pneumonia?," *Radiology,* p. 200847, 2020, doi: 10.1148/radiol.2020200847.

[50] E. Kalafat *et al.*, "Lung ultrasound and computed tomographic findings in pregnant woman with COVID-19," (in eng), *Ultrasound in obstetrics & gynecology : the official journal of the International Society of Ultrasound in Obstetrics and Gynecology,* Apr 6 2020, doi: 10.1002/uog.22034.

[51] Q. Y. Peng, X. T. Wang, L. N. Zhang, and G. Chinese Critical Care Ultrasound Study, "Findings of lung ultrasonography of novel corona virus pneumonia during the 2019-2020 epidemic," *Intensive Care Med,* Mar 12 2020, doi: 10.1007/s00134-020-05996-6.

[52] D. Buonsenso, A. Piano, F. Raffaelli, N. Bonadia, K. de Gaetano Donati, and F. Franceschi, "Point-of-Care Lung Ultrasound findings in novel coronavirus disease-19 pnemoniae: a case report and potential applications during COVID-19 outbreak," *European review for medical and pharmacological sciences,* vol. 24, no. 5, pp. 2776-2780, 2020-03 2020, doi: 10.26355/eurrev_202003_20549.

[53] F. Moro *et al.*, "How to perform lung ultrasound in pregnant women with suspected COVID-19 infection," *Ultrasound in obstetrics & gynecology : the official journal of the International Society of Ultrasound in Obstetrics and Gynecology,* 2020-Mar-24 2020, doi: 10.1002/uog.22028.

[54] M. C. Liszewski, S. Gorkem, K. S. Sodhi, and E. Y. Lee, "Lung magnetic resonance imaging for pneumonia in children," *Pediatric Radiology,* vol. 47, no. 11, pp. 1420-1430, Oct 2017, doi: 10.1007/s00247-017-3865-2.

[55] X. H. Yao *et al.*, "[A pathological report of three COVID-19 cases by minimally invasive autopsies]," *Zhonghua Bing Li Xue Za Zhi,* vol. 49, no. 0, p. E009, Mar 15 2020, doi: 10.3760/cma.j.cn112151-20200312-00193.

[56] L. Chen, X. Li, M. Chen, Y. Feng, and C. Xiong, "The ACE2 expression in human heart indicates new potential mechanism of heart injury among patients infected with SARS-CoV-2," *Cardiovasc Res,* Mar 30 2020, doi: 10.1093/cvr/cvaa078.

[57] R. M. Inciardi *et al.*, "Cardiac Involvement in a Patient With Coronavirus Disease 2019 (COVID-19)," *JAMA Cardiol,* Mar 27 2020, doi: 10.1001/jamacardio.2020.1096.

[58] X. Zou, K. Chen, J. Zou, P. Han, J. Hao, and Z. Han, "Single-cell RNA-seq data analysis on the receptor ACE2 expression reveals the potential risk of different human organs vulnerable to 2019-nCoV infection," *Front Med,* Mar 12 2020, doi: 10.1007/s11684-020-0754-0.

[59] H. Syrjala, M. Broas, P. Ohtonen, A. Jartti, and E. Paakko, "Chest magnetic resonance imaging for pneumonia diagnosis in outpatients with lower respiratory tract infection," *Eur Respir J,* vol. 49, no. 1, Jan 2017, doi: 10.1183/13993003.01303-2016.

[60] P. Konietzke *et al.*, "The value of chest magnetic resonance imaging compared to chest radiographs with and without additional lung ultrasound in children with complicated pneumonia," *PLoS One,* vol. 15, no. 3, p. e0230252, 2020, doi: 10.1371/journal.pone.0230252.

[61] A. Bernheim *et al.*, "Chest CT Findings in Coronavirus Disease-19 (COVID-19): Relationship to Duration of Infection," *Radiology,* pp. 200463-200463, 2020-Feb-20 2020, doi: 10.1148/radiol.2020200463.

[62] C. Huang *et al.*, "Clinical features of patients infected with 2019 novel coronavirus in Wuhan, China," *Lancet,* vol. 395, no. 10223, pp. 497-506, Feb 15 2020, doi: 10.1016/s0140-6736(20)30183-5.

[63] M. Chung *et al.*, "CT Imaging Features of 2019 Novel Coronavirus (2019-nCoV)," *Radiology,* vol. 295, no. 1, pp. 202-207, Apr 2020, doi: 10.1148/radiol.2020200230.

[64] D. Liu *et al.*, "Pregnancy and Perinatal Outcomes of Women With Coronavirus Disease (COVID-19) Pneumonia: A Preliminary Analysis," *AJR. American journal of roentgenology,* pp. 1-6, 2020-Mar-18 2020, doi: 10.2214/ajr.20.23072.

[65] J. C. L. Rodrigues *et al.*, "An update on COVID-19 for the radiologist - A British society of Thoracic Imaging statement," *Clinical radiology,* 2020-Mar-23 2020, doi: 10.1016/j.crad.2020.03.003.

[66] M.-Y. Ng *et al.*, "Imaging profile of the COVID-19 infection: radiologic findings and literature review," *Radiology: Cardiothoracic Imaging,* vol. 2, no. 1, p. e200034, 2020.

[67] R. Yang *et al.*, "Chest CT Severity Score: An Imaging Tool for Assessing Severe COVID-19," *Radiology: Cardiothoracic Imaging,* vol. 2, no. 2, p. e200047, 2020/04/01 2020, doi: 10.1148/ryct.2020200047.

[68] M. Li *et al.*, "Coronavirus Disease (COVID-19): Spectrum of CT Findings and Temporal Progression of the Disease," *Academic Radiology*, doi: 10.1016/j.acra.2020.03.003.

[69] F. Pan *et al.*, "Time Course of Lung Changes On Chest CT During Recovery From 2019 Novel Coronavirus (COVID-19) Pneumonia," *Radiology,* pp. 200370-200370, 2020-Feb-13 2020, doi: 10.1148/radiol.2020200370.

[70] Y. Wang *et al.*, "Temporal Changes of CT Findings in 90 Patients with COVID-19 Pneumonia: A Longitudinal Study," *Radiology,* pp. 200843-200843, 2020-Mar-19 2020, doi: 10.1148/radiol.2020200843.

[71] K.-C. Liu *et al.*, "CT manifestations of coronavirus

disease-2019: A retrospective analysis of 73 cases by disease severity," *European journal of radiology,* vol. 126, pp. 108941-108941, 2020-Mar-12 2020, doi: 10.1016/j.ejrad.2020.108941.

[72] X. Fang, M. Zhao, S. Li, L. Yang, and B. Wu, "Changes of CT Findings in a 2019 Novel Coronavirus (2019-nCoV) pneumonia patient," *QJM : monthly journal of the Association of Physicians,* 2020-Feb-19 2020, doi: 10.1093/qjmed/hcaa038.

[73] J. Chen *et al.*, "Deep learning-based model for detecting 2019 novel coronavirus pneumonia on high-resolution computed tomography: a prospective study," *medRxiv,* 2020.

[74] M. FANG *et al.*, "CT radiomics can help screen the coronavirus disease 2019 (COVID-19): a preliminary study," *SCIENCE CHINA Information Sciences,* vol. 63, no. 1674-733X, p. 172103, 2020, doi: https://doi.org/10.1007/s11432-020-2849-3.

[75] S. Wang *et al.*, "A deep learning algorithm using CT images to screen for Corona Virus Disease (COVID-19)," *medRxiv,* 2020.

[76] X. Xu *et al.*, "Deep Learning System to Screen Coronavirus Disease 2019 Pneumonia," *arXiv preprint arXiv:2002.09334,* 2020.

[77] S. Jin *et al.*, "AI-assisted CT imaging analysis for COVID-19 screening: Building and deploying a medical AI system in four weeks," *medRxiv,* 2020.

[78] Y. Song *et al.*, "Deep learning Enables Accurate Diagnosis of Novel Coronavirus (COVID-19) with CT images," *medRxiv,* 2020.

[79] C. Jin *et al.*, "Development and Evaluation of an AI System for COVID-19 Diagnosis," *medRxiv,* 2020.

[80] C. Zheng *et al.*, "Deep Learning-based Detection for COVID-19 from Chest CT using Weak Label," *medRxiv,* 2020.

[81] L. Li *et al.*, "Artificial Intelligence Distinguishes COVID-19 from Community Acquired Pneumonia on Chest CT," *Radiology,* p. 200905, 2020.

[82] F. Shi *et al.*, "Large-Scale Screening of COVID-19 from Community Acquired Pneumonia using Infection Size-Aware Classification," *arXiv preprint arXiv:2003.09860,* 2020.

[83] S. Wang *et al.*, "A Fully Automatic Deep Learning System for COVID-19 Diagnostic and Prognostic Analysis," *medRxiv,* 2020.

[84] W. Shi *et al.*, "Deep Learning-Based Quantitative Computed Tomography Model in Predicting the Severity of COVID-19: A Retrospective Study in 196 Patients," *SSRN Electronic Journal,* 01/01 2020, doi: 10.2139/ssrn.3546089.

[85] Z. Zhou, M. M. R. Siddiquee, N. Tajbakhsh, and J. Liang, "Unet++: A nested u-net architecture for medical image segmentation," in *Deep Learning in Medical Image Analysis and Multimodal Learning for Clinical Decision Support*: Springer, 2018, pp. 3-11.

[86] O. Ronneberger, P. Fischer, and T. Brox, "U-net: Convolutional networks for biomedical image segmentation," in *International Conference on Medical image computing and computer-assisted intervention*, 2015: Springer, pp. 234-241.

[87] O. Gozes *et al.*, "Rapid ai development cycle for the coronavirus (covid-19) pandemic: Initial results for automated detection & patient monitoring using deep learning ct image analysis," *arXiv preprint arXiv:2003.05037,* 2020.

[88] F. Shan *et al.*, "Lung Infection Quantification of COVID-19 in CT Images with Deep Learning," *arXiv preprint arXiv:2003.04655,* 2020.

[89] T.-Y. Lin, P. Dollár, R. Girshick, K. He, B. Hariharan, and S. Belongie, "Feature pyramid networks for object detection," in *Proceedings of the IEEE conference on computer vision and pattern recognition*, 2017, pp. 2117-2125.

[90] G. Huang, Z. Liu, L. Van Der Maaten, and K. Q. Weinberger, "Densely connected convolutional networks," in *Proceedings of the IEEE conference on computer vision and pattern recognition*, 2017, pp. 4700-4708.

[91] S. Wang *et al.*, "Predicting EGFR mutation status in lung adenocarcinoma on computed tomography image using deep learning," *European Respiratory Journal,* vol. 53, no. 3, p. 1800986, 2019.

[92] S. Wang *et al.*, "Deep learning provides a new computed tomography-based prognostic biomarker for recurrence prediction in high-grade serous ovarian cancer," *Radiotherapy and Oncology,* vol. 132, pp. 171-177, 2019.

[93] X. Zhao *et al.*, "The characteristics and clinical value of chest CT images of novel coronavirus pneumonia," *Clinical Radiology,* vol. 75, no. 5, pp. 335-340, May 2020, doi: 10.1016/j.crad.2020.03.002.